





that includes re-surveyed well positions and deviation surveys. Each stratigraphic top was re-picked with particular focus paid to the reservoir units and all the dipmeter data was QC'd and subsequently re-interpreted. With a solid database established and the stratigraphy understood (Figure 2), the TSTs could be calculated to be used as an essential aspect of 3D model building.

The process of model building directly in 3D is illustrated in Figure 4. It begins with building panels at all drilled formation tops within 500 m above and below the reservoir, using the correct dip and azimuth interpreted for that depth (Figure 4A). On their own these panels provide a limited amount of information concerning the structure of the Toro reservoir. However when combined with structural information obtained throughout the wellbore a more complete picture of the reservoir structure can be built and the higher the deviation of the well-bore the more valuable the information represented by these panels becomes.

The second stage is to use the known stratigraphy and TST information to project each panel up from beneath the Toro or downwards from the overburden to reservoir level, thereby creating a web of Toro panels around the well (Figure 4B). Thus a highly deviated well that drilled beyond the reservoir unit can produce several panels that represent the Toro reservoir despite only intersecting it once. This process was repeated for all of the key horizons in upwards of 70 wells and sidetracks in the Kutubu Field, focusing on producing as many panels that represent the reservoir unit as the data would allow.

In the third stage of this process, the panels are widened until they intersect other panels and they are cut at the intersection. Where the panels do not intersect they are left unjoined, allowing for discontinuities and offsets in the model, which are later interpreted as faults. This method reveals structural geometries away from the wellbore and discontinuities or offsets in horizons (Figure 4C). Faults are introduced to the model after offsets are observed in the horizon data (Figure 4D). The fourth and final stage of model building is to join and smooth each of the panels, tidy to faults and to combine with the 2D section interpretation discussed in the next section (Figure 4D and Figure 6).

### **3D Methodology – Cross-sections**

In areas of less dense well data, the 3D panel method is not applicable and we resorted to the traditional construction of cross-sections. Firstly, three key sections were constructed along the regional seismic lines and were balanced and restored and also forward-modelled to check their validity (see Kutubu section in Hill et al., 2015). A further 18 local and detailed sections dip-cross-sections were constructed well within 25° (<10% geometrical error) of the inferred tectonic transport direction, NE to SW, using Move™ software. For each section, 3D structural domains were established within which the plunge was consistent based on the available surface and well data. These plunges were used to project dips and formation tops onto the section. Typically data were projected less than 1 km and usually <500 m. In areas where the 3D panel model overlapped the section it was 'sliced' along the section and given priority. The key sections were used as a guide to interpret the remaining 18 sections, by projecting the interpretation down-plunge onto the section and adjusting it to fit the constraining data.

In the Hedinia Anticline, the seismic data are of very poor quality and there are few wells as it hosts the gas-cap which remained untouched whilst the oil was being produced, reinjecting the gas. Here different structural interpretations were possible and it became important to use the observed structural style along strike in PNG to choose between them. Using inferred TSTs, the base of the Miocene Darai Limestone was projected from surface data and tied to the available wells. However, the surface geology map shows lower Darai TMD4 juxtaposed against

upper Darai TMD3/2 across a fault (Figure 1). Lamerson (1990) interpreted this to be a backthrust, which thickens the Darai Limestone and pushes down the crest at Toro reservoir level. However, along strike in the Mananda Anticline a similar structure was defined by four wells and drilled by two sidetracks (Keenan and Hill, 2015) and found to be an old normal fault that had been decapitated by the main thrust. Furthermore, the Cretaceous section at Mananda was ~20% thinner in the footwall of the normal fault, which further elevated the Toro reservoir. This interpretation for Hedinia is shown on Figure 5 and is consistent with thin Cretaceous section encountered in wells along strike in the Hedinia Anticline.

Once the three key sections and 18 local sections were drawn, the faults were constructed in 3D by triangular interpolation followed by smoothing. Then the horizons were similarly constructed, but were cut-off at the faults. For the whole model, the initial hydrocarbon contacts were drawn on for each horizon to check that the positions of saddles and sealing faults made sense geologically. In general, few alterations were needed, but structure and faults were adjusted between wells which were known to have different contacts. A view of the final 3D model with translucent cross-cutting faults is shown in Figure 6.

### Conclusions

- Given the 3D complexity of the structure and the paucity of good quality seismic data, the only way to constrain the interpretation was by building a detailed 3D geologic model.
- Building the model directly in 3D from structural panels was both efficient and reliable in areas of dense well data
- In areas of low well density, many serial sections were constructed in the tectonic transport direction, with the interpretation guided by key regional balanced and restored sections
- Where multiple interpretations were possible, the structural style observed along strike in the Papuan Fold Belt was used to select the most likely solution
- Overall the Kutubu oil and gas fields comprise a double-humped 'pop-up' structure with the Hedinia Anticline above the SW-verging Hedinia Thrust and the Iagifu Anticline above the NE-verging Iagifu Backthrust.
- The syncline between the Hedinia and Iagifu anticlines is interpreted to lie along a minor normal fault active in the Cretaceous and reactivated more recently. The fault system accounts for oil-water contacts in the Digimu and for thinner Ieru Formation on the Hedinia Anticline.
- The Iagifu Anticline is very well constrained by abundant borehole data and moderate quality seismic data. It is offset by a down-to-the-NW cross-cutting fault that separates the SE-nose which has a 217 m oil column from the NW-nose that has no oil column.
- The Hedinia Anticline is less well constrained due to a paucity of boreholes and very poor seismic data so the 3D model was largely built from closely-spaced geologic cross-sections. Based on analogies with the Mananda Anticline, the Crestal Fault in the Darai Limestone was interpreted to be a normal fault with thin Cretaceous section in the footwall, producing the interpreted Toro reservoir crest. The alternate Lamerson (1990) backthrust interpretation may also be considered.
- The final 3D model was consistent with all initial hydrocarbon contacts and explained them in a geologically reasonable way.

## References Cited

Bradey, K., K. Hill, D. Lund, N. Williams, T. Kivior, and N. Wilson, 2008, Kutubu Oil Field, Papua New Guinea - A 350 MMbl Fold Belt Classic, *in* J.E. Blevin, B.E. Bradshaw, and C. Uruski (eds.), Eastern Australasian Basins Symposium III, Petroleum Exploration Society of Australia, Special Publication, p. 239-246.

Hill, K.C., R.H. Wightman, and L. Munro, 2015, Structural Style in the Eastern Papuan Fold Belt, From Wells, Seismic, Maps and Modelling: AAPG/SEG International Conference & Exhibition, Melbourne, Australia, September 13-16, 2015, Search and Discovery Article #30433 (2015). [http://www.searchanddiscovery.com/documents/2015/30433hill/ndx\\_hill.pdf](http://www.searchanddiscovery.com/documents/2015/30433hill/ndx_hill.pdf)

Hornafius, J.S., and R.E. Denison, 1993, Structural Interpretations Based on Strontium Isotope Dating of the Darai Limestone, Papuan Fold Belt, Papua New Guinea, *in* G.J. Carman and Z. Carman (eds.), Petroleum Exploration in Papua New Guinea: Proceedings of the First PNG Petroleum Convention, Port Moresby, p. 313-324.

Keenan, S.E., and K.C. Hill, 2015, The Mananda Anticline, Papua New Guinea: A Third Oil Discovery, Appraisal Programme and Deep Potential: AAPG/SEG International Conference & Exhibition, Melbourne, Australia, September 13-16, 2015, AAPG Search and Discovery Article #10803 (2015). [http://www.searchanddiscovery.com/documents/2015/10803keenand/ndx\\_keenan.pdf](http://www.searchanddiscovery.com/documents/2015/10803keenand/ndx_keenan.pdf).

Lamerson, P.R., 1990, Evolution and Structural Interpretations in Iagifu/Hedina Field, Papua New Guinea, *in* G.J. Carman and Z. Carman (eds.), Petroleum Exploration in Papua New Guinea: Proceedings of the First PNG Petroleum Convention, Port Moresby, p. 283-300.

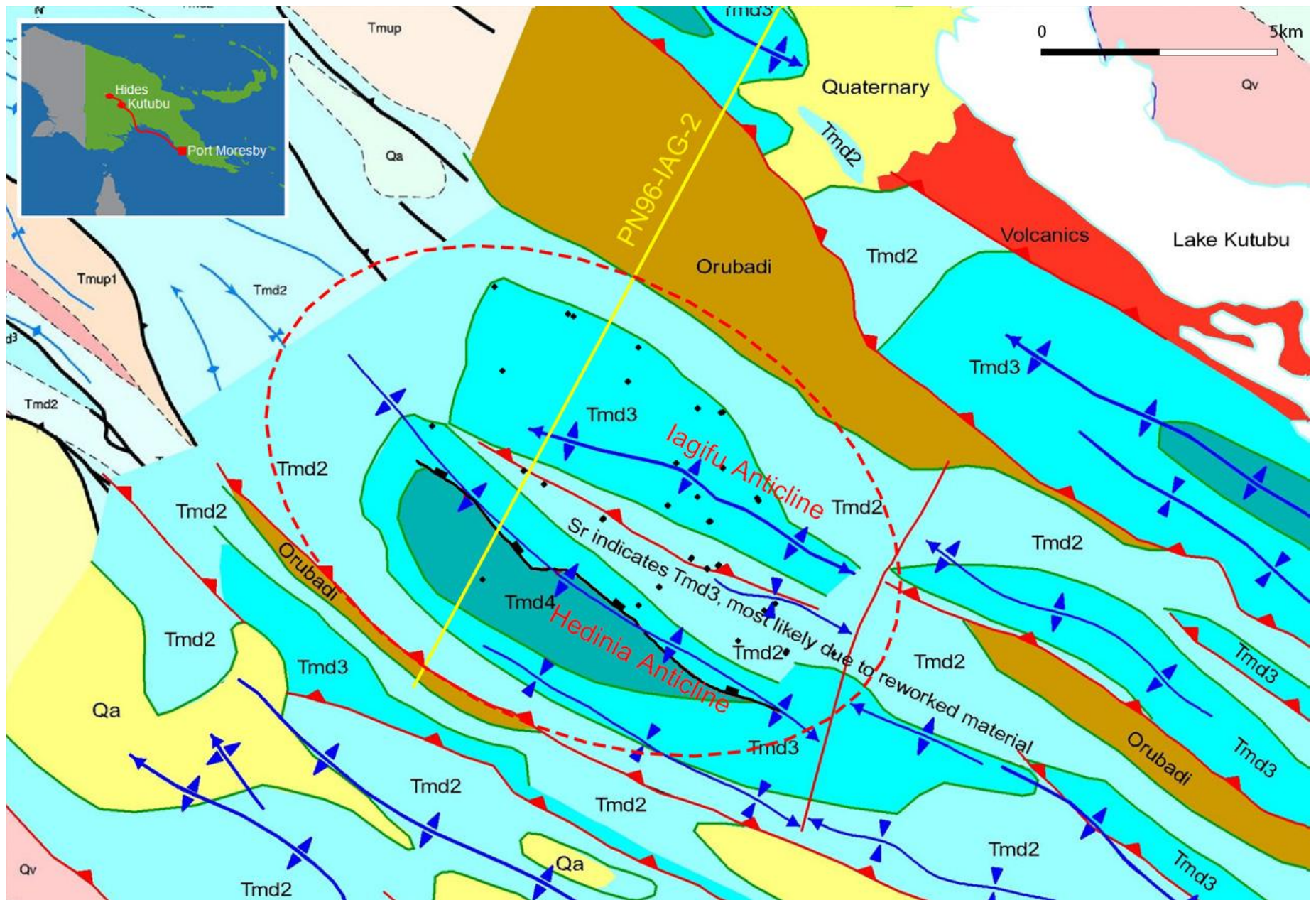


Figure 1. Surface geology map of the Kutubu anticline (within red dashed line) showing line of cross section in Figure 5 (in yellow); inset is a location map showing the Kutubu field. Units as in Figure 2.

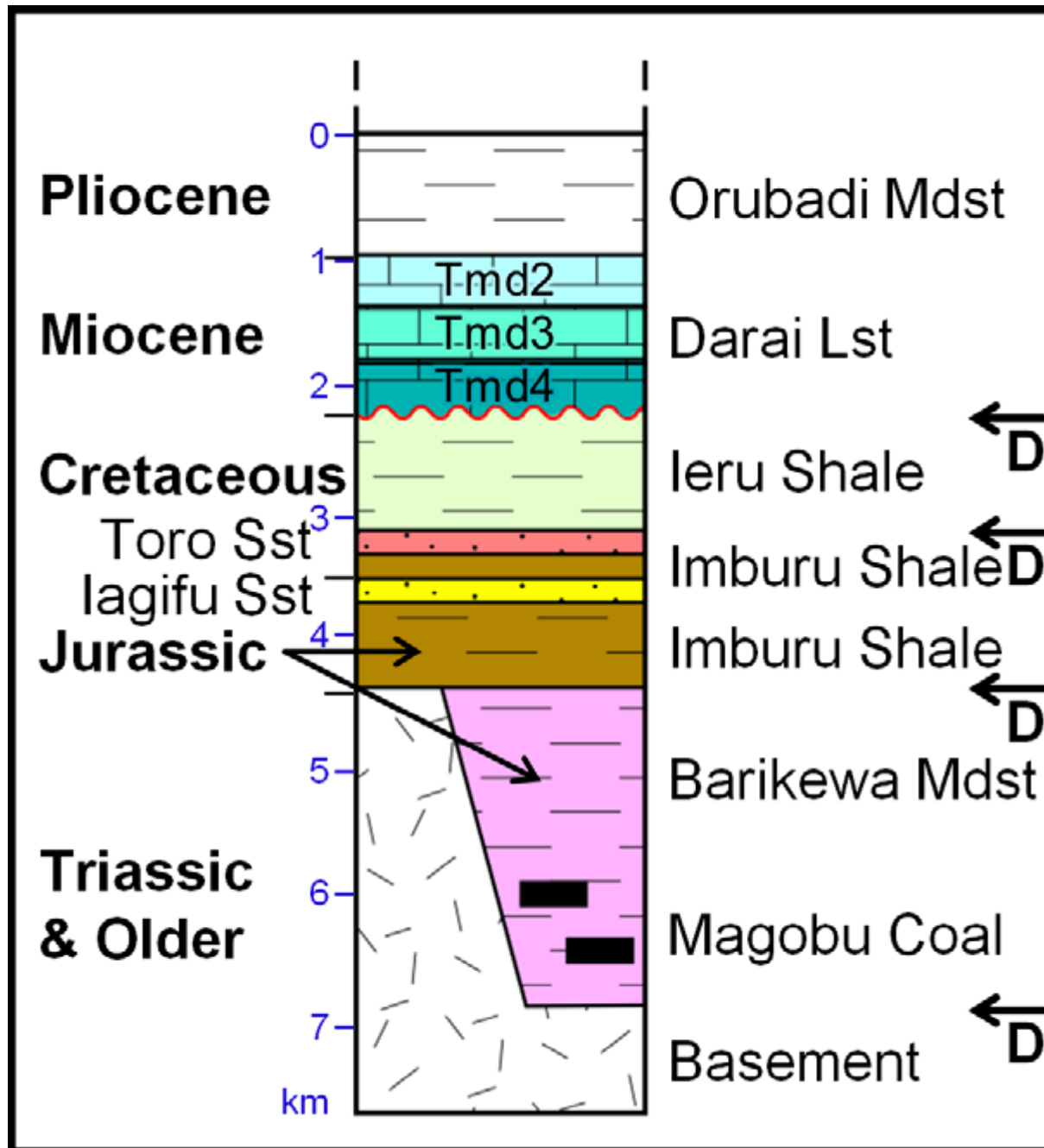


Figure 2. The stratigraphic column at the Kutubu anticline.

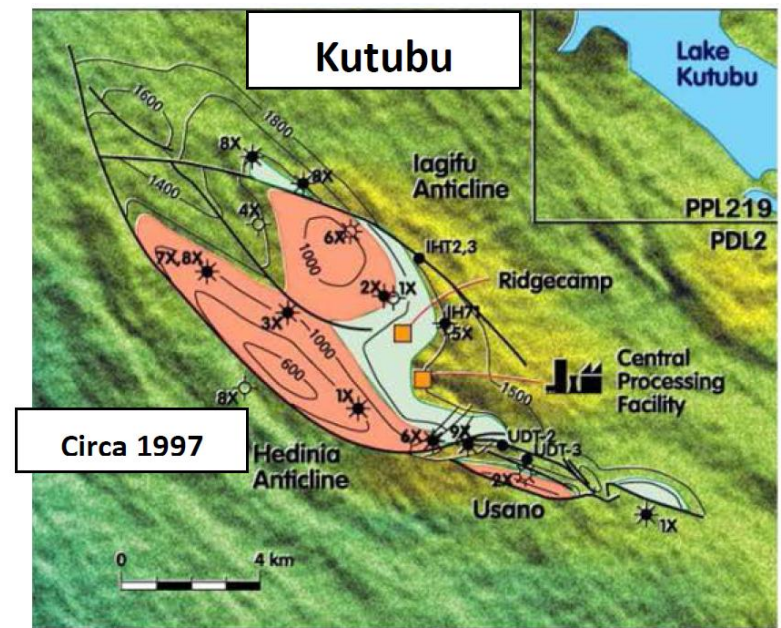
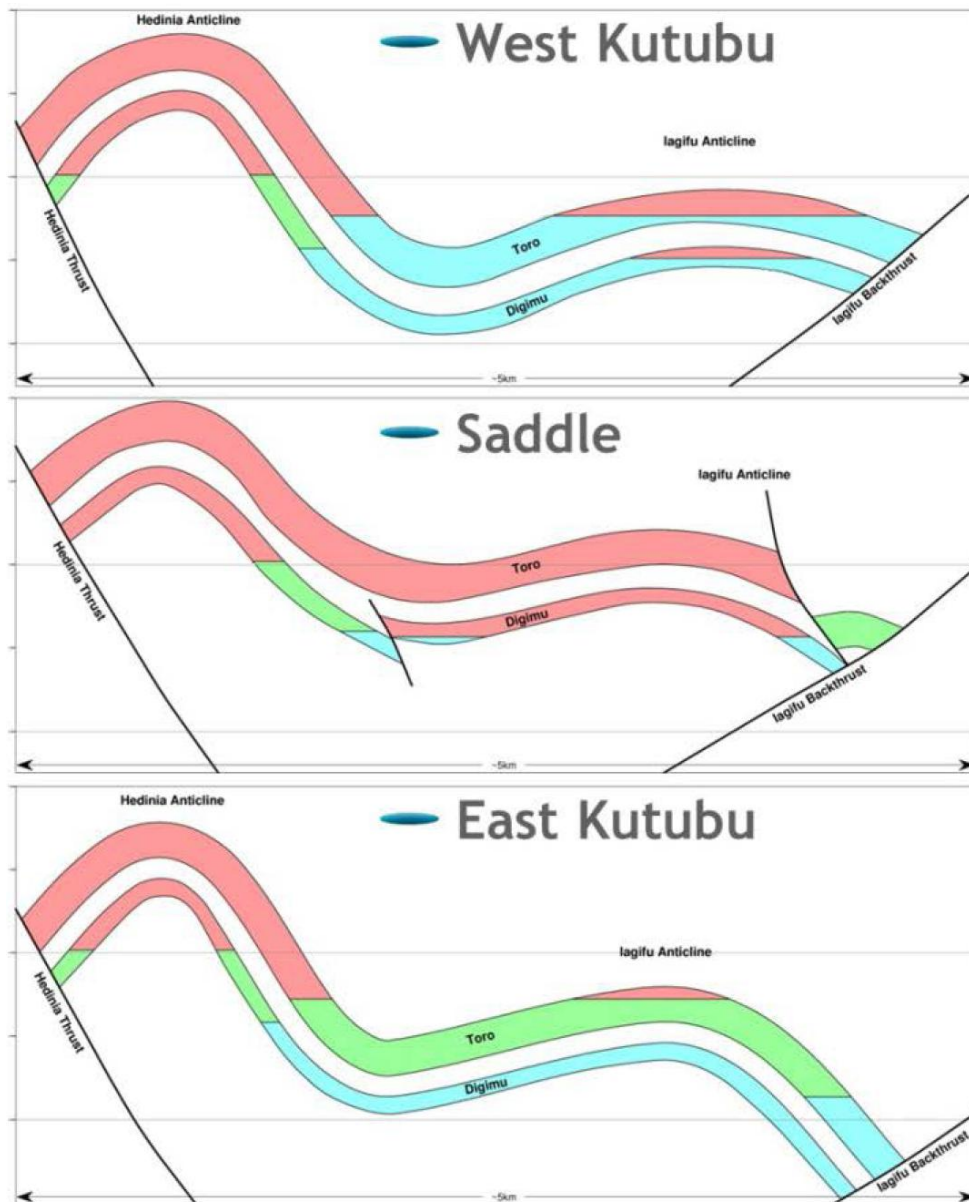


Figure 3. Schematic cross sections of the Kutubu anticline with different fluid contacts across the field; a map of the Kutubu anticline with fluid contacts.



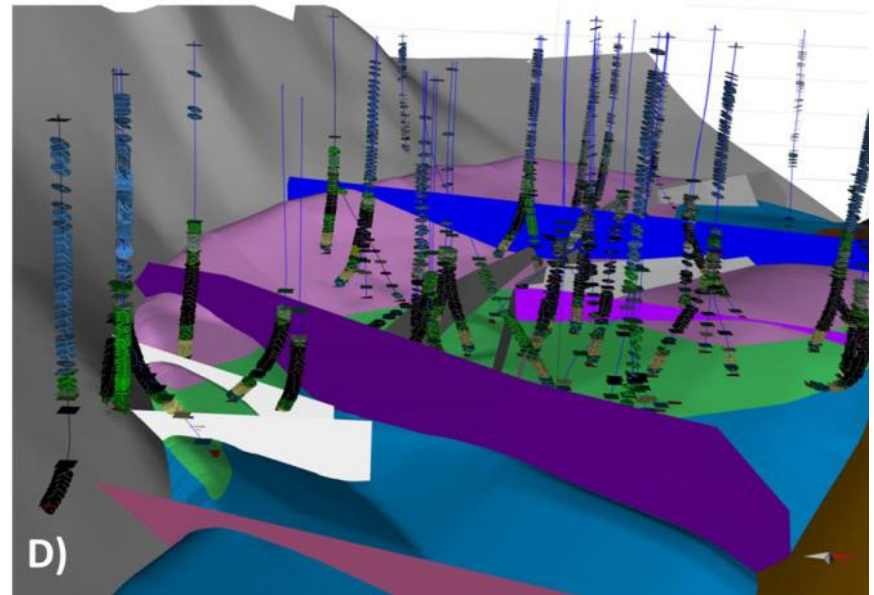
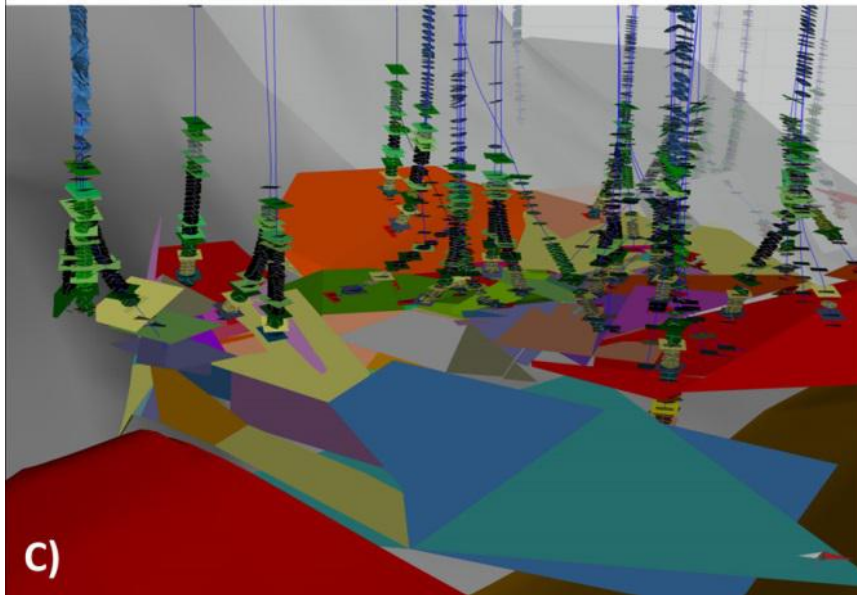
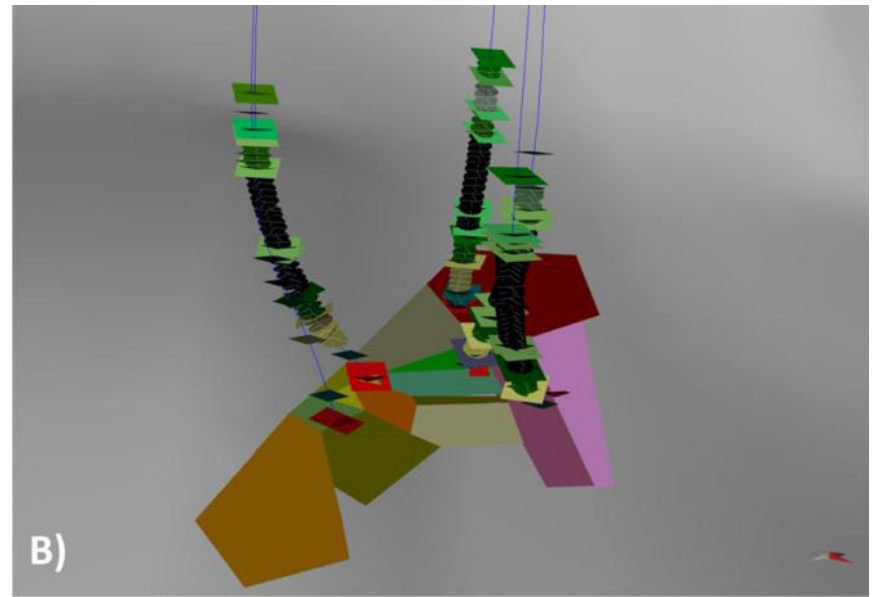
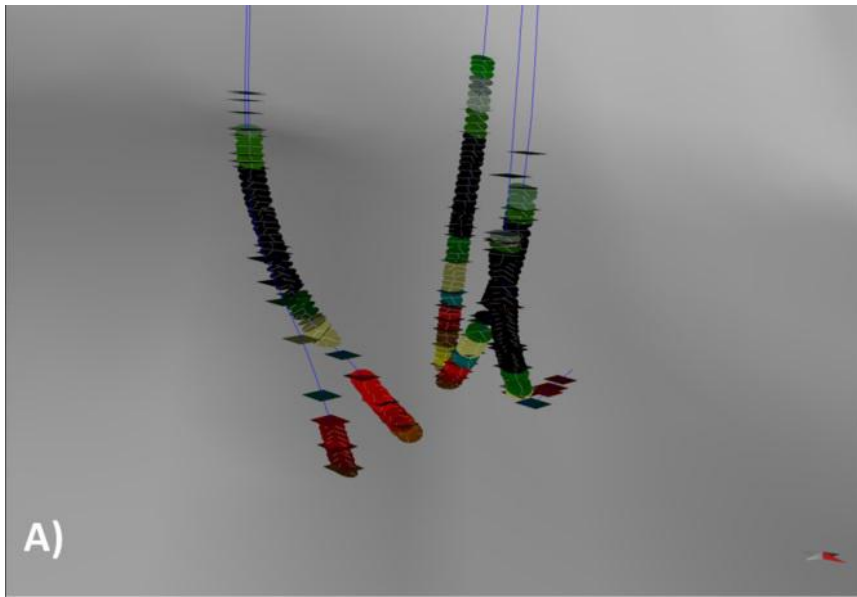


Figure 4. A) Five deviated wells with tops (square) and dips (round) coloured by formation, B) Top Toro panels projected from adjacent formations on a selection of wells, C) Top Toro panels for all wells and sidetracks, D) Top Toro panels joined, smoothed and tidied to faults and coloured by fluid content, pink=gas, green = oil and blue = water.

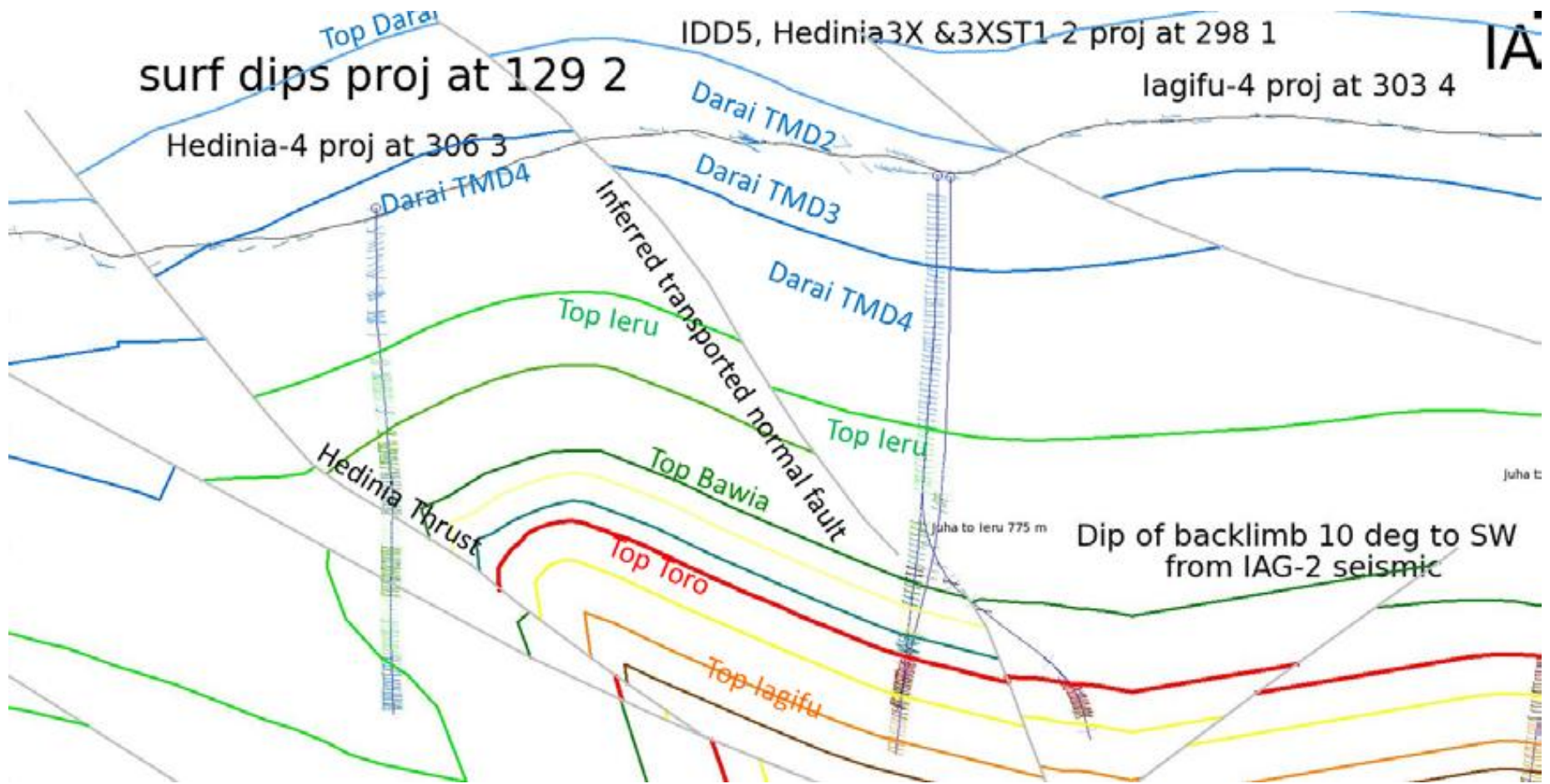


Figure 5. Interpretation of the Crestal Fault on the Hedinia Anticline assuming a normal fault as in the crest of the Mananda anticline (Keenan et al, this volume).

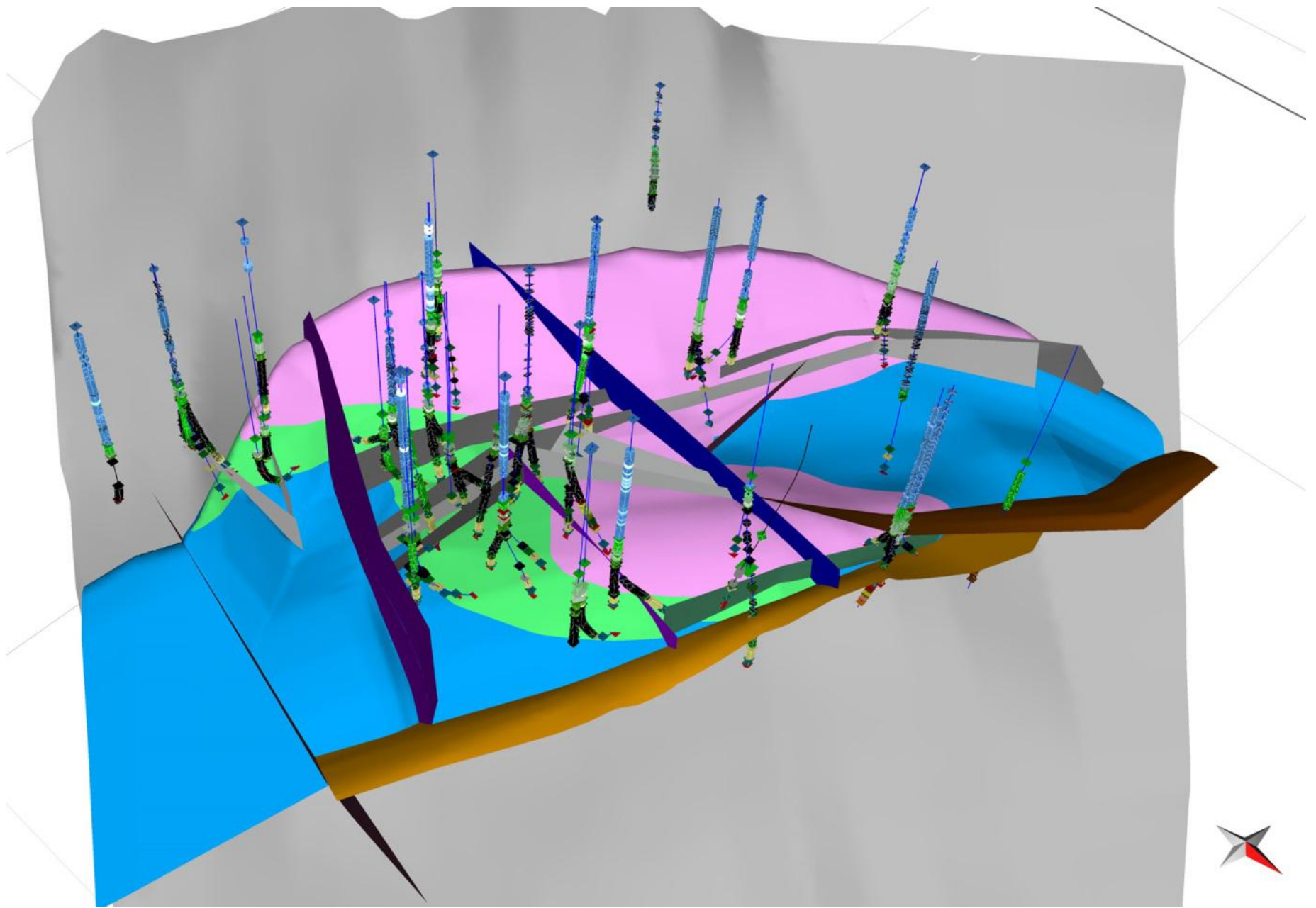


Figure 6. 3D perspective view of the final top Toro surface and main faults in the 3D model, looking towards the SW. Pink is gas, green is oil and blue is water.